# Strain-Dependent Differences in Sensitivity to Myopia-Inducing Stimuli in Guinea Pigs and Role of Choroid

Liqin Jiang,[1,2] Mariana B. Garcia,[3] David Hammond,[4] Dinasha Dahanayake,[1] and Christine F. Wildsoet[1]

[1]Berkeley Myopia Research Group, Vision Science Program and School of Optometry, University of California, Berkeley, California, United States
[2]Singapore Eye Research Institute, Singapore
[3]Exponent, Menlo Park, California, United States
[4]Faculty of Health, School of Medicine–Optometry, Deakin University, Victoria, Australia

Correspondence: Mariana B. Garcia, Exponent, 149 Commonwealth Drive, Menlo Park, CA 94025, USA; mariana.b.garcia@gmail.com.

LJ and MBG are joint first authors.

Submitted: July 25, 2018
Accepted: February 4, 2019

Citation: Jiang L, Garcia MB, Hammond D, Dahanayake D, Wildoset CF. Strain-dependent differences in sensitivity to myopia-inducing stimuli in guinea pigs and role of choroid. *Invest Ophthalmol Vis Sci*. 2019;60:1226–1233. https://doi.org/10.1167/iovs.18-25365

**Purpose.** To investigate differences in sensitivity to myopia-inducing stimuli of two strains of pigmented guinea pigs.

**Methods.** Eleven-day-old animals (New Zealand [NZ], $n = 24$ and Elm Hill strains [EH], $n = 26$) wore either a +2 or −2 diopter (D) lens over one eye and a plano lens over the fellow eye for 5 days; other 10-day-old EH ($n = 9$) and 7-day-old NZ ($n = 9$) animals were monocularly form-deprived (FD) for 28 days. Choroidal thickness and axial length were measured using A-scan ultrasonography at baseline and after 1 and 5 days for optical defocus treatments, and at baseline and after 28 days for the FD treatment. Refractive errors were measured by retinoscopy. Choroids of untreated animals were also evaluated using spectral-domain optical coherence tomography.

**Results.** One day of optical defocus induced bidirectional (optical sign-dependent) choroidal responses in EH animals only ($P < 0.01$). Similar responses were detected in NZ animals after 5 days ($P < 0.01$), with concordant spherical equivalent refraction changes ($P < 0.01$). Compared with NZ animals, EH animals developed minimal myopia with FD after 28 days ( −4.58 ± 0.97 vs. −0.69 ± 0.75 D for NZ versus EH, $P < 0.001$). Yet, EH animals showed paradoxical choroidal thickening, 20 ± 9 vs. −8 ± 8 μm for EH versus NZ, $P < 0.001$. Untreated EH animals also had significantly thicker choroids than NZ animals (147 ± 19 vs. 132 ± 16 μm, $P < 0.05$), with well-defined layering.

**Conclusions.** As previously reported in chicks, guinea pigs show strain-related differences in response to myopia-inducing stimuli. The finding of a thicker, multilayered choroid in the strain showing decreased sensitivity to FD is provocative, suggesting a possible protective role of the choroid.

Keywords: guinea pigs, experimental myopia, choroid, emmetropization, sensitivity

Emmetropization represents an active and highly regulated developmental process by which the eye grows in length to approximately match the power of its refracting elements. Failures in emmetropization give rise to refractive errors. Myopia falls into the latter category and is characterized by an eye that is too long for its refractive power.[1,2] The worldwide distribution of myopia has been trending upward, with myopia now affecting 22% of the world's population[3] and already at epidemic levels in industrialized East Asian countries.[4] The development of myopia in young children allows more time for it to progress to high levels, increasing the risks of complicating ocular pathologies, such as choroidal neovascularization, retinoschisis, and myopic maculopathy.[5,6] Of potential relevance to the current study, significant regional- and population-based differences in the risk of myopia in children have been reported,[7] with one recent study reporting predominantly mild hyperopia in Norwegian adolescents (i.e., 57%), in sharp contrast to the high myopia prevalence figures for the same age group in East Asia.[8]

In young eyes, whether they be human or animal, both lenticular and "choroidal" accommodation can alter the refractive state. The first case involves changes in the power of the crystalline lens,[9] whereas the latter involves changes in the thickness of the choroid, which has the effect of moving the retinal photoreceptors relative to the ocular plane of focus.[10] The modulation of choroidal thickness is now recognized as a key feature of active emmetropization, mechanistically linked to blood flow dynamics, the tone of nonvascular smooth muscle, and locally synthesized, space-filling macromolecules such as proteoglycans.[11,12] In young chicks (*Gallus gallus*), a widely used model for studies of eye growth regulation, sustained increases in choroidal thickness are coupled to slowed scleral growth and ocular elongation, the converse being true for choroidal thinning.[11,13] The net refractive error outcomes are hyperopic and myopic shifts in refractive errors, respectively. These observations inform the conclusion that the choroid and sclera together play important roles in the homeostatic regulation of refractive errors.[14,15] The choroid appears to play an early key role in the emmetropiza-

tion response, with measurable thickness changes in response to imposed optical defocus within a matter of a few hours, while the response of the sclera is much slower, taking days.[14,16–18]

Guinea pigs (*Cavia porcellus*) have emerged as an important mammalian model of myopia, combining the advantage of a fibrous-only sclera, as in primate eyes, with ease of housing and husbandry. Published studies have established their responsiveness to commonly used myopia-inducing visual manipulations, specifically, to form deprivation with diffusers[19,20] and imposed hyperopic defocus using negative lenses.[17,21] Except for a small number of studies involving albino guinea pigs, pigmented animals have been used in studies of emmetropization and myopia.[17,19–26] As characteristic of most infant animals, the refractive errors reported for pigmented guinea pigs at birth typically exhibit a hyperopic bias (e.g., +5.22 ± 0.65 diopters [D][24] and +4.40 ± 0.40 D[22]), with lower levels of hyperopia in older, 30-day-old animals (e.g., +3.03 ± 1.69 D[24] and +0.7 D[22]).

The study described here introduces an Elm Hill (EH) strain of pigmented guinea pig that is novel in three ways: animals retain relatively high levels of hyperopia on completion of developmental emmetropization, they are relatively unresponsive to both myopia-inducing negative lenses and diffusers, and they have relatively thick multilayered choroids. Comparisons are made in all cases with another pigmented strain of guinea pig of New Zealand origin, whose ocular profile was considered normal by comparison with published literature from other myopia research laboratories.[17,20,22,24]

## Materials and Methods

### Animals

Both strains of guinea pigs used in the current study were pigmented and bred on-site. In the case of the strain designated as "Elm Hill" (EH), breeders were purchased from a commercial supplier (Elm Hill Labs, Chelmsford, MA, USA). In the case of the strain designated as "New Zealand" (NZ), breeders were obtained from the University of Auckland, New Zealand. Groupings for breeding were restricted to unrelated animals, based on on-site records. For both strains, pups were weaned at 5 days of age and housed as single-sex pairs in transparent plastic wire-top cages, in a room with 12-hour/12-hour light/dark cycle with an average floor luminance of approximately 160 to 180 lux. Animals had free access to water and vitamin C–supplemented food and received fresh fruit and vegetables three times a week as diet enrichment. All animal care and treatments in this study conformed to the ARVO Statement for the Use of Animals in Ophthalmic and Vision Research. Experimental protocols were approved by the Animal Care and Use Committee of the University of California, Berkeley, USA.

### Visual Manipulation Paradigms

Both optical defocusing "spectacle" lenses and form-depriving diffusers were used in this study. Both treatments were applied monocularly. Diffuser and lens designs, and attachment protocols were adapted from those implemented in chicks.[27] Diffusers (transmittance 15% ± 1%) were made from sheets of white styrene (Midwest Products Co., Hobart, IN, USA), hot-molded into semicircular domes and attached to Velcro supports, as described for the lenses. Lenses were custom-made from polymethylmethacrylate (Valley Contax, Springfield, OR, USA), with a back optic radius of 8 mm and an overall diameter of 17 mm, and included powers of −2 and +2 D, as well as plano (0 D). The lenses were affixed to hook Velcro supports along with a 2-cm-diameter plastic washer (to impart rigidity) (Seastrom Manufacturing, Twin Falls, ID, USA), using a UV-curing glue (Norland Optical Adhesive #68; Norland Products, Cranbury, NJ, USA). To attach these devices (lenses or diffusers) to the guinea pigs, rings of loop Velcro were symmetrically affixed to the fur surrounding the eyes of guinea pigs, using a small amount of gel cyanoacrylate glue (SureHold Plastic Surgery, SureHold, Chicago, IL, USA).

For all treatments, animals were monitored at least hourly during the 12-hour light cycle to ensure that the lenses/diffusers remained in place. Lenses were cleaned 1 to 2 times daily; diffusers were cleaned as necessary.

### Experiments

The design of experiments, including visual manipulations and sample sizes, are summarized in Table 1. As emmetropization in guinea pigs is normally complete by approximately 3 weeks of age,[22,24] this study was limited to guinea pigs that were 11 days old or younger on entry. In short-term monocular optical defocus treatments, contralateral fellow eyes were fitted with plano lenses instead of being left uncovered, to control for any potentially confounding ocular effects of lens fitting, albeit subtle.

**Optical Defocus.** To examine the sensitivity of animals to optical defocus, lenses were fitted to 11-day-old guinea pigs and worn for 5 days. Eleven NZ animals were fitted with −2 D lenses and 13 animals were fitted with +2 D lenses. Thirteen EH animals were fitted with −2 D lenses and 13 animals, with +2 D lenses.

**Form Deprivation.** To examine the sensitivity of animals to form deprivation, diffusers were applied monocularly, with contralateral eyes left untreated as controls. They were fitted when the guinea pigs were 7 or 10 days old (NZ and EH animals, respectively), and worn for 28 days ($n = 9$ for each group). This extended treatment period allowed for the possibility that apparent strain-related differences in sensitivity to form deprivation reflected differences in the rate of response rather than a lack of sensitivity, and capitalizes on the open-loop nature of the form deprivation treatment.

**Choroid Evaluation.** Because early baseline measurements for the above studies suggested inherent differences in the thickness of the choroids in the two strains of guinea pigs, a further study of untreated 11-day-old animals of both strains ($n = 8$ for each strain) was undertaken, using A-scan ultrasonography to evaluate their normal (untreated) on-axis choroidal thickness and in vivo imaging to compare the morphology of their choroids.

### Measurements of Refractive Error and Ocular Dimensions

Refractive error data were collected over the experimental period using streak retinoscopy and are reported as spherical equivalent refractive errors (average of the results for the two principal meridians). In the longer-term form deprivation experiment, cycloplegic refractions were measured on awake animals 30 minutes after instillation of 1% cyclopentolate hydrochloride (Bausch & Lomb, Rochester, NY, USA), on experimental days 0 (baseline), 14, and 28. In the short-term optical defocus experiment, retinoscopy was performed on awake noncycloplegic animals, because complete recovery from the effects of cyclopentolate usually takes approximately 24 hours, with potential confounding effects of the responses to the treatments over this period. Measurements were made on experimental days 0 (baseline), 1, and 4.

**Table 1.** Summary of Visual Manipulations and Animal Numbers Used in Short-Term (5 Days) Monocular Optical Defocus and Longer-Term (28 Days) Form Deprivation Experiments

| | Defocus Experiment* | | Deprivation Experiment† | |
|---|---|---|---|---|
| | EH | NZ | EH | NZ |
| Treatments | −2, +2 D lenses | −2, +2 D lenses | Diffusers | Diffusers |
| Age of initiation, d | 11 | 11 | 10 | 7 |
| Sample sizes | 13, 13 | 11, 13 | 9 | 9 |

* Fellow eyes covered with plano lenses.
† Fellow eyes left uncovered.

Axial ocular dimensional data were collected using high-frequency A-scan ultrasonography (~10 μm resolution) under isoflurane anesthesia (1–2% in oxygen). Axial length was calculated by adding together the axial dimensions of the anterior chamber, crystalline lens, and vitreous chamber. In the longer-term form deprivation experiment, measurements were made before (day 0), and at the end of the 28-day wearing period. In the short-term optical defocus experiment, measurements were performed on experimental days 0, 1, and 4. Measurements on individual animals were conducted at the same time of day to prevent any possible confounding effects of diurnal ocular growth rhythms.[28] Each measurement comprised an average of at least seven scans.

The choroids of both strains were subject to additional comparative analysis, using high-resolution spectral-domain optical coherence tomography (SD-OCT; Bioptigen Envisu R-Series, Morrisville, NC, USA). Animals were first anesthetized with a ketamine/xylazine cocktail (27/0.6 mg/kg body weight). Cross-sectional images of the posterior ocular fundus were captured to include the optic nerve head (ONH) as a reference landmark, thereby allowing the alignment of related images captured over time for analyses of changes in choroidal thickness. Choroidal analyses were restricted to the visual streak region, which is approximately 2.5 ONH diameters (~700 μm) away from the center of the ONH (Fig. 1). OCT scans consisted of 70 B-scans by 700 A-scans, with 30 frames per B-scan and a 2.6 × 2.6-mm-wide field of view. All OCT scans were performed between 1:00 and 3:00 PM to minimize effects of diurnal variations in choroidal thickness on collected data. Choroidal thickness data were obtained from collected images using the in-built calipers. In addition, an ImageJ (http://imagej.nih.gov/ij/; provided in the public domain by the National Institutes of Health, Bethesda, MD, USA) macro (developed by Dr. Benjamin E. Smith, Vision Science Group, University of California, Berkeley) was used to measure choroidal vessel area, as well as total interstitial area in captured images (available at https://github.com/Llamero/Manually_measure_vessel_diameter-Macro). The ratio of total vessel area to interstitial area was then calculated. As the more peripheral aspects of images are most prone to optical distortion, only the middle one-third of each cross-sectional image was analyzed. In total, eight images from each of eight animals of each strain were analyzed.

### Statistical Analyses

Treatment effects are generally expressed as interocular (treated eye − control eye) differences, normalized to baseline (pretreatment) values. All data are reported as mean ± standard error. Unpaired two-tailed *t*-tests were applied to compare the results for the two guinea pig strains. For all data analyses, *P* values less than 0.05 were considered statistically significant.

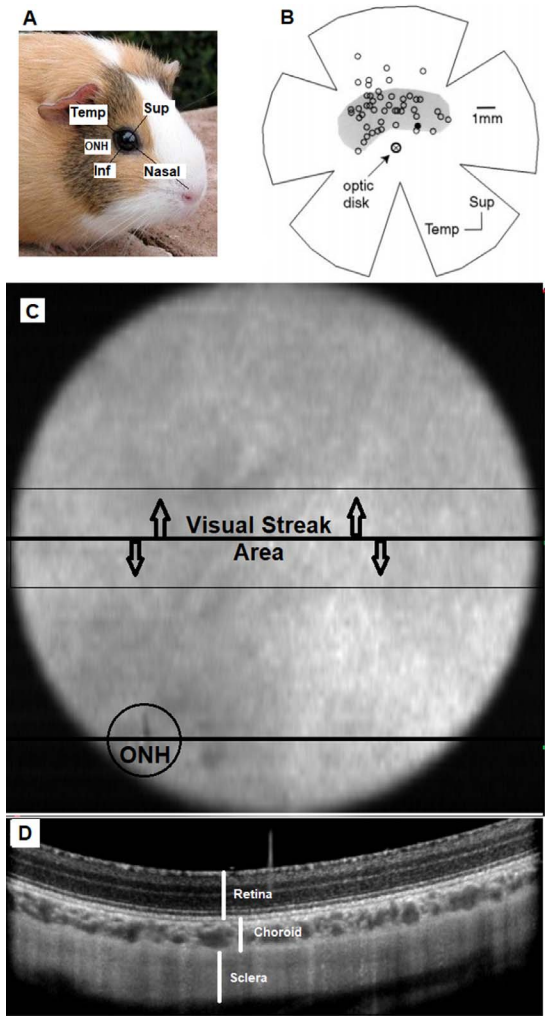


**Figure 1.** Ocular landmarks and representative images from OCT imaging of the right eye of an 11-day-old guinea pig. (**A**) Guinea pig photo with superimposed ocular meridians (temporal – nasal and superior – inferior). (**B**) Schematic of flattened retina showing location of visual streak (shaded region), in relation to the optic nerve head (ONH) from Demb et al., 1999. (**C**) En face fundus image of guinea pig right eye, as visualized with OCT; the ONH (276 ± 27 μm average diameter) is located in the inferior temporal quadrant; visual streak, approximately demarcated by thin black lines (highlighted with *arrows*), is 700 μm above the ONH. (**D**) OCT cross-sectional image showing the fundus layers in the visual streak region (at the location delineated by the thick black reference line in [**C**]).

## Results

### Strain-Related Differences in Refractive Error and Choroidal Responses to Short-Term Optical Defocus

After just 1 day of optical defocus, EH but not NZ animals exhibited optical sign-dependent, bidirectional changes in choroidal thickness, measured by A-scan ultrasonography, although bidirectional response patterns were evident after 5 days of optical defocus in NZ animals (Fig. 2A). Specifically, in EH animals, choroidal thinning was seen in response to the −2 D lenses (−16 ± 5 μm), which was much larger than the

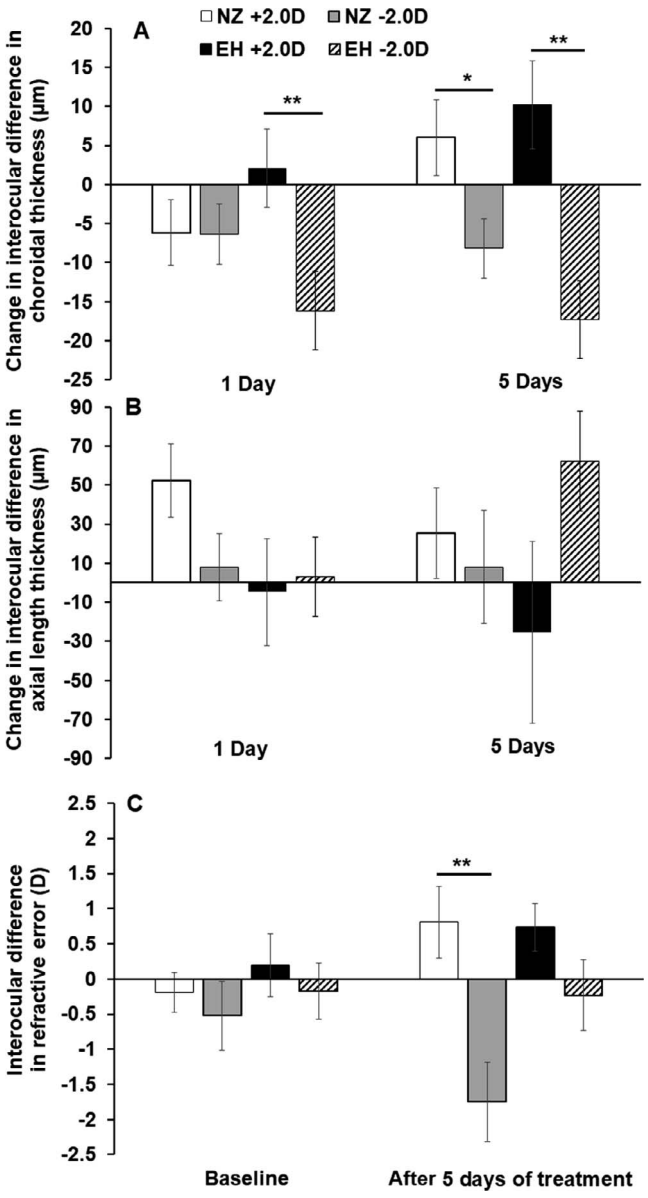


FIGURE 2. Responses to −2 D and +2 D lens treatments in NZ and EH guinea pigs, shown as interocular differences (treated eye − control eye). Choroidal (**A**) and axial length (**B**) changes after 1 and 5 days of lens wear, normalized to baseline values. Interocular differences in refractive error (**C**) at baseline and after 5 days of lens wear. $^{*}P < 0.05$; $^{**}P < 0.01$.

thickening response elicited by the +2 D lenses (+2 ± 5 µm). The thinning response in EH animals was also approximately double the magnitude of, and significantly different from, the changes induced by the −2 D lenses in the NZ animals ($P < 0.01$, unpaired *t*-test). Furthermore, over this short treatment period, NZ animals exhibited choroidal thinning, regardless of the sign of imposed defocus (i.e., –6 ± 4 µm versus –6 ± 4 µm for −2 D and +2 D lenses, respectively). However, after 5 days of optical defocus, the choroids of NZ animals treated with +2 D lenses were significantly thicker (+6 ± 5 µm), than the choroids of eyes treated with −2 D lenses, which remained thinned (–8 ± 4 µm) ($P < 0.05$, unpaired *t*-test). The choroids of the EH animals continued to exhibit distinct bidirectional responses that were also significantly different from each other (–2 D versus +2 D: –17 ± 6 µm versus +10 ± 6 µm, $P < 0.01$, unpaired *t*-test). In summary, the EH guinea pigs showed early, enduring bidirectional choroidal responses to positive and negative lenses, whereas for NZ guinea pigs, the thickening response to positive lenses emerged more slowly.

The axial length changes induced by the optical defocus treatments are shown in Figure 2B. Although none of the changes (i.e., after either 1 or 5 days of optical defocus) proved to be statistically significant for either strain, curiously over the time frame of this study only the EH strain showed an apparent trend of increased axial elongation after 5 days of optical defocus imposed with negative lenses.

The EH and NZ animals also exhibited different responses with regard to induced changes in refractive error (Fig. 2C). After 5 days of optical defocus treatment, NZ animals exhibited a hyperopic shift in response to the +2 D lens treatment (+0.81 ± 0.51 D) and a myopic shift with the −2 D lens treatment (–1.75 ± 0.56 D), these different responses being statistically significant ($P = 0.003$, unpaired *t*-test). In contrast, the changes in refractive error in EH animals were smaller for the −2 D lens treatment (–0.23 ± 0.50 D) and not significantly different from those induced by the +2 D lens treatment (+0.73 ± 0.34 D, $P = 0.13$, unpaired *t*-test). The apparent mismatch between changes in refractive error and axial length suggest optical contributions to the refractive error changes recorded in NZ animals, a point taken up again in the discussion.

## Strain-Related Differences in Responses to Form Deprivation

NZ and EH guinea pigs showed significant differences in their sensitivity to the myopia-genic effect of form deprivation, with EH animals proving to be relatively insensitive. This point is well illustrated by the contrasting changes in axial length and refractive error in NZ versus EH guinea pigs after 28 days of form deprivation, as shown in Figure 3. At the end of the treatment period, interocular differences in axial length for EH animals were small and significantly different from the much larger changes recorded for NZ animals (normalized mean interocular differences: 24 ± 34 µm versus 174 ± 42 µm, respectively, $P = 0.01$, unpaired *t*-test). Accordingly, the myopic shifts in refractive errors for EH animals were also significantly smaller than the shifts observed in NZ animals (mean interocular differences: –0.69 ± 0.75 D versus –4.58 ± 0.97 D, respectively, $P = 0.006$, unpaired *t*-test).

The two strains showed opposite patterns for choroidal responses to form deprivation (Fig. 4). After 28 days of form deprivation, the NZ animals showed the typical choroidal thinning (–8 ± 8 µm), whereas the choroids of EH animals thickened (20 ± 9 µm). Similar trends are evident in the fellow untreated eyes of the two strains, suggestive of interocular yoking of these choroidal responses, although the differences were only significant for treated eyes ($P < 0.05$, unpaired *t*-test).

## Choroidal Thickness and Vascular Network Morphology Differences Between Strains

The choroids of untreated EH guinea pigs were significantly thicker than those of age-matched NZ guinea pigs, as measured by A-scan ultrasonography (Fig. 5A; 147 ± 19 µm versus 132 ±16 µm, $P = 0.04$, unpaired *t*-test). Interestingly EH animals also had thicker retinas compared with those of NZ animals as measured by A-scan ultrasonography (114 ± 5 µm versus 106 ± 5 µm, $P < 0.01$, unpaired *t*-test, Fig. 5A). The above difference in choroidal thickness is consistent with data extracted from OCT images (Table 2), although the equivalent differences derived from OCT images did not reach statistical significance. For both strains, choroidal thickness was relative-

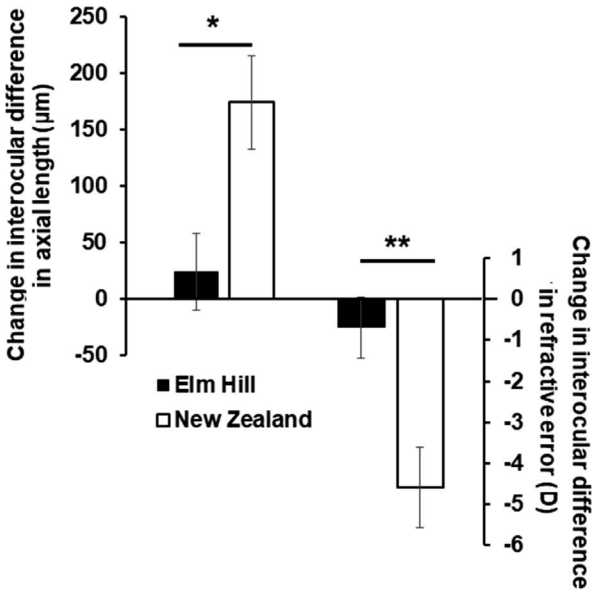


FIGURE 3. Interocular differences (treated eye − control eye), normalized to baseline values, in axial length (*left*) and refractive error (*right*) for EH and NZ guinea pigs after 28 days of form deprivation. $^{*}P = 0.02$, $^{**}P = 0.006$.

ly uniform within the visual streak, as confirmed with measurements at least three different locations within relevant OCT scans. The variability in the OCT-derived choroidal thickness data, expressed in terms of the standard deviation of repeated measurements from individual eyes, is less than 5% of the average choroidal thickness (i.e., 4.1 ± 2.4 μm for EH animals and 4.1 ± 2.6 μm for NZ animals).

The OCT images also revealed the thicker choroids of EH animals to be apparently multilayered (Fig. 5C), compared with the unilayered, thinner choroids of NZ animals (Fig. 5B). Analyses of the vascular network morphology of presumed choroidal blood vessels revealed the choroids of NZ guinea pigs to have significantly fewer and smaller vessels compared with those of EH guinea pigs. Data from age-matched NZ and EH animals are shown in Figure 6 and summarized in Table 2. For NZ and EH animals, 69 and 114 blood vessels were identified and outlined respectively, with their corresponding summed cross-sectional areas being 19,671 $\mu m^2$ and 26,905 $\mu m^2$. The overall thickness of the choroids used in these analyses are 79 ± 5 μm and 128 ± 9 μm for NZ and EH animals respectively. Note, however, that the ratios of total vessel area to interstitial area are similar, 0.48 ± 0.07 for NZ animals and 0.45 ± 0.05 for EH animals.

## DISCUSSION

Although there are previous reports of strain-related differences in the responses of chicks to visual manipulations known to affect early eye growth regulation,[29,30] we believe this is the first study to report such a difference in a mammalian model. Specifically, we found a commercially available strain of pigmented guinea pig, the EH strain, to be minimally sensitive to both form deprivation and hyperopic defocus imposed by negative lenses, at least in refractive error terms. Conversely, the NZ strain showed the expected myopic changes in response to these treatments. In studies aimed at understanding the origin of the different responses, the EH strain was found to have a naturally thicker and structurally more complicated choroid compared with the "sensitive" NZ strain.

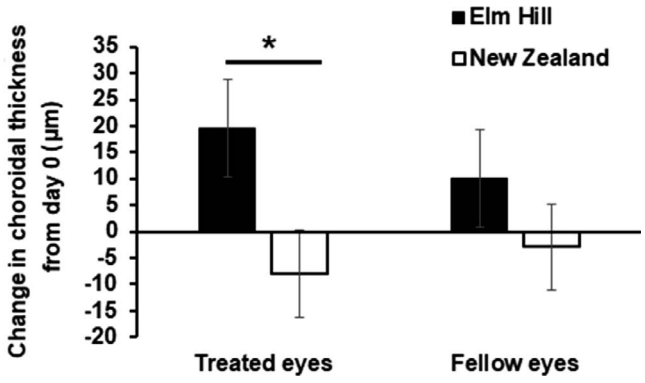


FIGURE 4. Change in choroidal thickness for EH and NZ guinea pigs after 28 days of form deprivation. The choroids of treated eyes thickened in EH animals and thinned in NZ animals, with similar but smaller changes in fellow untreated eyes. $^{*}P < 0.05$.

Differences in the choroidal response patterns to both lens (optical defocus) and form deprivation treatments were also observed. We have tentatively attributed the reduced sensitivity to myopia-genic manipulations of the EH animals to their thicker choroids, and in the following discussion, speculate on underlying mechanisms, as well as consider the potential broader significance of these observations.

The important role of the choroid in early eye growth regulation has been well demonstrated in the chick, as described in a widely cited review.[11] Early studies in chicks reported choroidal thinning linked to accelerated axial elongation in response to myopia-genic visual manipulations, such as form deprivation and negative lenses. Conversely, previous studies also reported choroidal thickening in response to manipulations that slow axial elongation, such as positive lenses. Related studies in monkeys, guinea pigs, and humans revealed similar trends.[16,17,23,31] Together these findings suggest an important role of the choroid in ocular growth regulation and emmetropization. However, there remains much to be understood about the signal pathways regulating such choroidal thickness changes, the mechanisms underlying the thickness changes, and interrelationship between choroidal and scleral changes during early eye growth.[13] As explanations for how the innate thickness and/or structure of the choroid might influence the susceptibility of eyes to myopia, documented here as an insensitivity to form deprivation, we offer the following possibilities: mechanical buffering, diffusion barrier, a role for a network of choroidal melanocytes.

Thicker choroids may serve as a mechanical buffer against scleral expansion[11] and/or a more effective diffusion barrier to scleral-directed growth modulatory molecules being released from the RPE.[13,32] Consistent with the latter notion, OCT images obtained in our study clearly showed the thicker choroids of the EH animals to be multilayered, with more large-sized vessels compared with the choroids of NZ animals. Although the ratios of vessel to interstitial area were not different between the two strains, nonetheless, in absolute terms, the thicker choroids of EH strain necessarily must have more interstitial (stromal) tissue, which includes collagen and elastic fibers, fibroblasts, nonvascular smooth muscle cells, and numerous melanocytes in the case of EH animals. This increased amount of interstitial tissue may impede diffusion of RPE-derived growth modulatory molecules, in addition to any effects of differences in the choroidal vasculature on the clearance of diffusing molecules, thereby altering the scleral response to growth modulatory signals generated in the retina.

The third possibility offered above involves choroidal melanocytes, which were reported to be connected by gap

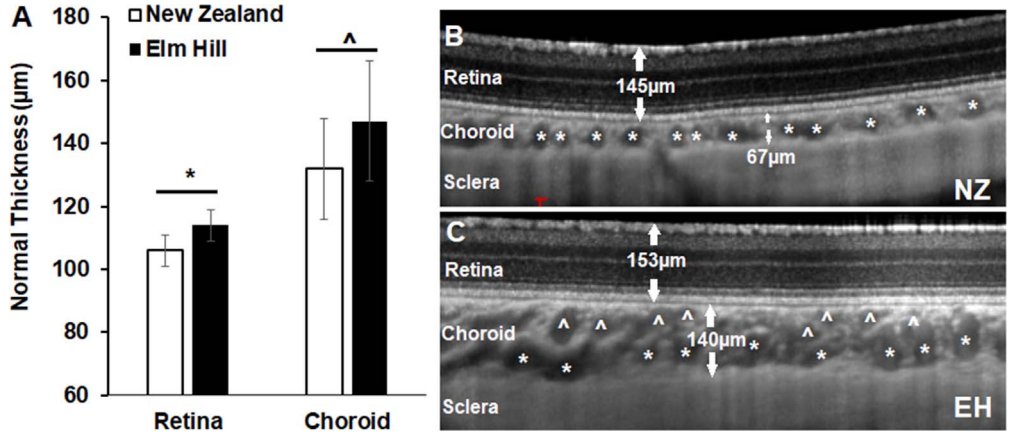


FIGURE 5. Retinal and choroidal thicknesses measured by A-scan ultrasonography in 11-day-old EH and NZ guinea pigs (**A**), and by OCT imaging in an NZ animal (**B**) and an EH animal (**C**), as examples. $^{*}P < 0.01$, $^{\wedge}P = 0.04$.

junctions in one study in guinea pigs, suggesting that they function as a network.[33] Qualitatively, the choroids of the EH strain appeared more heavily pigmented than those of the NZ strain (observation during tissue dissection by authors). At this time, relatively little is known about the function of choroidal melanocytes, apart from minimizing light scatter. However, recent studies reported evidence that choroidal melanocytes both synthesize and secrete L-DOPA, the precursor of dopamine.[26,34] Given the extensive literature linking dopamine with eye growth regulation, this recent finding raises the possibility that melanocytes are directly involved in eye growth regulation.

Although the preceding discussion offered explanations for how differences in choroidal thickness and/or structure might contribute to differences in the effects on the sclera and thus eye size of myopia-generating growth signals from the retina, the paradoxical thickening of the choroids with form deprivation in EH animals cannot be similarly explained. Either choroidal structural differences between the two strains make their choroids differentially sensitive to growth regulatory molecules released from RPE and/or there are fundamental strain-related differences in the retinal growth modulatory signals generated in response to form deprivation.

Interestingly, data from both chick and monkey models suggest differences in signal pathways regulating form deprivation- and defocus-induced myopia.[35–38] At this time, we cannot rule out a retinal contribution to the strain-related differences in sensitivity to form deprivation reported here. In a study involving chicks, choroidal thickness was found to be predictive of normal eye growth but not experimentally altered (form deprivation-induced) growth.[39] That the EH strain showed the expected choroidal thickness changes in response to imposed optical defocus pattern suggests that retinal decoding of imposed optical defocus was not impaired.

TABLE 2. Choroidal Thickness and Morphological Parameters, Including Blood Vessel and Interstitial Areas, Derived Using In-Built Instrument Calipers and ImageJ, Respectively, Applied to Eight OCT Images Collected From Eight Guinea Pigs of Each Strain (NZ and EH)

| | NZ | EH |
|---|---|---|
| Choroidal thickness, µm | 79 ± 5 | 128 ± 9* |
| Total numbers of vessels in sampled area | 69 | 114 |
| Total interstitial area, µm$^2$ | 5146 ± 200 | 8131 ± 611* |
| Ratio of vessel to interstitial area, µm$^2$ | 0.48 ± 0.07 | 0.45 ± 0.06 |

* $P < 0.01$; significant difference between two strains.

Consistent with results from previous Australian-based studies involving guinea pigs,[17] both strains showed bidirectional, optical sign-dependent choroidal response patterns, albeit with different temporal profiles. Indeed, the choroids of EH animals showed greater thinning in response to the negative defocusing lenses than their NZ counterparts, although their refractive errors changed minimally. The poor correspondence between axial length and refractive error changes in the optical defocus groups also raise the possibility of differences in the anterior segments of these two strains and potential corneal involvement, although curvature data were not collected in this study. However, we also cannot rule out the possibility of a signal transmission abnormality downstream from the choroid (at the level of sclera).

Advances in SD-OCT imaging now allow for noninvasive profiling the ocular choroid, including assessment of its thickness and regional variations. It is also possible to visualize its structural morphology,[40,41] which for human eyes includes two vascular layers, Sattler's and Haller's layers, as defined by medium- and large-sized vessels respectively. In the context of the current study, cross-sectional studies in humans have linked the relative thickness of these vessel layers to refractive errors, with hyperopes having the thickest and myopes, the thinnest layers.[41,42] In yet another study, myopic children were reported to have thinner choroids than

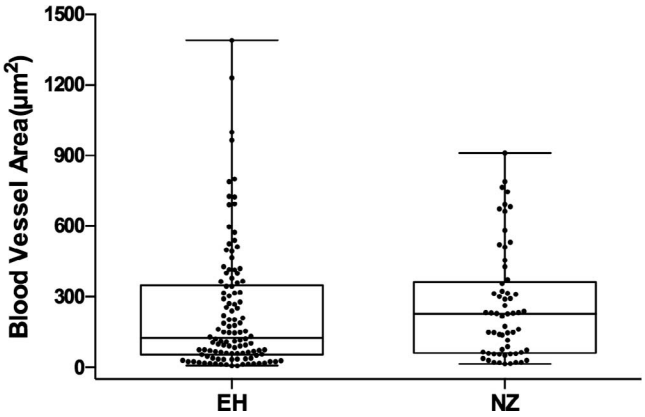


FIGURE 6. Cross-sectional areas of blood vessels (*y*-axis) and their distribution (*x*-axis) quantified from a total of eight choroidal images for each strain. On average, NZ animals have far fewer choroidal vessels per imaged section than EH animals (69 vessels versus 114 vessels), although the NZ animals recorded a larger median vessel diameter.

Table 3. Comparison of Choroidal Thickness Data Representing Approximately Age-Matched Emmetropic Children of Different Ethnicities

| Ethnicity | Age, y | Refractive Error, D | Choroidal Thickness, µm | Sample Size |
|---|---|---|---|---|
| Chinese[47] | 9.9 ± 1.2 | +0.18 ± 0.26 | 253 ± 58 | 91 |
| Japanese[48] | 7.9 ± 3.1 | −0.04 ± 1.96 | 260 ± 57 | 100 |
| Indian[49] | 11.9 ± 3.4 | −0.50 ± 1.09 | 311 ± 45 | 136 |
| American[50] | 10.2 ± 3.4 | +0.11 ± 1.83 | 319 ± 53 | 91 |
| Australian[51] | 8.2 ± 1.9 | +0.05 ± 0.21 | 330 ± 65 | 194 |

non-myopes, with the rate of developmental choroidal thickening in children being inversely related to the rate of eye elongation (i.e., the fastest growing eyes showed less thickening).[43] Finally, a comparison of choroidal thickness data extracted from studies encompassing age-matched emmetropic children of different ethnicities revealed differences that appear to be correlated with myopia prevalence figures. Specifically, ethnicities with higher myopia prevalence tended to have thinner choroids (Table 3). Nonetheless, the causal connection between choroidal thickness and refractive error remains to be resolved for humans and there are likely multiple risk factors for myopia.[44]

Results from recent accommodation studies in humans strongly suggest that the thickness of the human choroid is modulated by optical defocus,[45,46] just as in animal models, including the guinea pig models used on the current study. For example, young adults measured during accommodation tasks were found to show significant choroidal thinning for the highest 6 D task.[45] In another study, choroidal thinning was reported in response to monocular −2 D contact lenses worn for 60 minutes.[46]

Through the work reported here, we found that the bidirectionality of the choroidal responses to imposed optical defocus was preserved in both guinea pig strains. However, there were differences in the temporal dynamics, with faster thickening taking place in the strain that ultimately proved to be insensitive to form deprivation (EH strain). It is interesting to speculate that children showing the fastest myopia progression may have altered choroidal response dynamics and/or a signaling abnormality, as raised above.

Our observations of a relationship between baseline choroidal thickness and susceptibility to myopia development, as well as related differences in choroidal morphology, may be translatable to a clinical setting. As noted earlier, it has become feasible to image the choroid at high resolution with SD-OCT, at least in cooperative subjects. As this technology is advancing rapidly, it soon should be possible to screen and subsequently track choroidal changes in younger children along with their refractive error to further address the relationship between choroidal thickness and/or morphology and sensitivity to myopia in children.

In conclusion, we have documented strain-dependent differences in choroidal thickness and morphology in guinea pigs, which seem to be linked to differences in developmental emmetropization responses. Although it is acknowledged that myopia is a complex disease, with likely genetic and environmental influences, results linking a relatively thick multilayered choroid with an apparent insensitivity to form deprivation myopia provide strong argument for further investigations into the potential influence of the choroidal structure and dynamics on myopia susceptibility in children.

## Acknowledgments

Supported by NIH/National Eye Institute R01EY12392 (CFW).

Disclosure: **L. Jiang**, None; **M.B. Garcia**, None; **D. Hammond**, None; **D. Dahanayake**, None; **C.F. Wildoset**, None

## References

1. Stone RA, Khurana TS. Gene profiling in experimental models of eye growth: clues to myopia pathogenesis. *Vision Res*. 2010;50:2322–2333.
2. Curtin B. *The Myopias: Basic Science and Clinical Management*. Philadelphia: Harper & Row; 1985.
3. Holden B, Sankaridurg P, Smith E, Aller T, Jong M, He M. Myopia, an underrated global challenge to vision: where the current data takes us on myopia control. *Eye*. 2014;28:142–146.
4. Jones D, Luensmann D. The prevalence and impact of high myopia. *Eye Contact Lens*. 2012;38:188–196.
5. Morgan IG, Ohno-Matsui K, Saw SM. Myopia. *Lancet*. 2012; 379:1739–1748.
6. Curtin BJ, Iwamoto T, Renaldo DP. Normal and staphylomatous sclera of high myopia. An electron microscopic study. *Arch Ophthalmol*. 1979;97:912–915.
7. Holden BA, Fricke TR, Wilson DA, et al. Global prevalence of myopia and high myopia and temporal trends from 2000 through 2050. *Ophthalmology*. 2016;123:1036–1042.
8. Hagen L, Gjelle J, Arnegard S, Pedersen H, Gilson S, Baraas R. Prevalence and possible factors of myopia in Norwegian adolescents. *Sci Rep*. 2018;8:13479.
9. Pour HM, Kanapathipillai S, Zarrabi K, Manns F, Ho A. Stretch-dependent changes in surface profiles of the human crystalline lens during accommodation: a finite element study. *Clin Exp Optom*. 2015;98:126–137.
10. Wallman J, Wildsoet C, Xu A, et al. Moving the retina: choroidal modulation of refractive state. *Vision Res*. 1995;35: 37–50.
11. Nickla DL, Wallman J. The multifunctional choroid. *Prog Retin Eye Res*. 2010;29:144–168.
12. Nickla DL, Wildsoet C, Wallman J. Compensation for spectacle lenses involves changes in proteoglycan synthesis in both the sclera and choroid. *Curr Eye Res*. 1997;16:320–326.
13. Summers JA. The choroid as a sclera growth regulator. *Exp Eye Res*. 2013;114:120–127.
14. Wallman J, Winawer J. Homeostasis of eye growth and the question of myopia. *Neuron*. 2004;43:447–468.
15. Norton TT, Rada JA. Reduced extracellular matrix in mammalian sclera with induced myopia. *Vision Res*. 1995; 35:1271–1281.
16. Hung LF, Wallman J, Smith EL III. Vision-dependent changes in the choroidal thickness of macaque monkeys. *Invest Ophthalmol Vis Sci*. 2000;41:1259–1269.
17. Howlett MH, McFadden SA. Spectacle lens compensation in the pigmented guinea pig. *Vision Res*. 2009;49:219–227.
18. Wildsoet C, Wallman J. Choroidal and scleral mechanisms of compensation for spectacle lenses in chicks. *Vision Res*. 1995;35:1175–1194.
19. Howlett MH, McFadden SA. Form-deprivation myopia in the guinea pig (*Cavia porcellus*). *Vision Res*. 2006;46:267–283.
20. Lu F, Zhou X, Zhao H, et al. Axial myopia induced by a monocularly-deprived facemask in guinea pigs: a non-invasive and effective model. *Exp Eye Res*. 2006;82:628–636.

Investigative Ophthalmology & Visual Science

21. Jiang L, Zhang S, Schaeffel F, et al. Interactions of chromatic and lens-induced defocus during visual control of eye growth in guinea pigs (*Cavia porcellus*). *Vision Res*. 2014;94:24–32.
22. Howlett MH, McFadden SA. Emmetropization and schematic eye models in developing pigmented guinea pigs. *Vision Res*. 2007;47:1178–1190.
23. Lu F, Zhou X, Jiang L, et al. Axial myopia induced by hyperopic defocus in guinea pigs: a detailed assessment on susceptibility and recovery. *Exp Eye Res*. 2009;89:101–108.
24. Zhou X, Qu J, Xie R, et al. Normal development of refractive state and ocular dimensions in guinea pigs. *Vision Res*. 2006; 46:2815–2823.
25. Jiang L, Long K, Schaeffel F, et al. Disruption of emmetropization and high susceptibility to deprivation myopia in albino guinea pigs. *Invest Ophthalmol Vis Sci*. 2011;52:6124–6132.
26. Jiang L, Zhang S, Chen R, et al. Effects of the tyrosinase-dependent dopaminergic system on refractive error development in guinea pigs. *Invest Ophthalmol Vis Sci*. 2018;59: 4631–4638.
27. Choh V, Lew MY, Nadel MW, Wildsoet CF. Effects of interchanging hyperopic defocus and form deprivation stimuli in normal and optic nerve-sectioned chicks. *Vision Res*. 2006;46:1070–1079.
28. Nickla DL, Wildsoet C, Wallman J. The circadian rhythm in intraocular pressure and its relation to diurnal ocular growth changes in chicks. *Exp Eye Res*. 1998;66:183–193.
29. Troilo D, Li T, Glasser A, Howland HC. Differences in eye growth and the response to visual deprivation in different strains of chicken. *Vision Res*. 1995;35:1211–1216.
30. Schmid K, Wildsoet C. Breed- and gender-dependent differences in eye growth and form deprivation responses in chick. *J Comp Physiol A*. 1996;178:551–561.
31. Wang D, Chun RK, Liu M, et al. Optical defocus rapidly changes choroidal thickness in schoolchildren. *PLoS One*. 2016;11:e0161535.
32. Zhang Y, Wildsoet CF. RPE and choroid mechanisms underlying ocular growth and myopia. *Prog Mol Biol Transl Sci*. 2015;134:221–240.
33. Matsusaka T, Takemura K, Takada T. The lamina suprachoroidocapillaris of the guinea pig choroid confirmed by the rapid freezing and freeze-substitution method. *J Electron Microscop (Tokyo)*. 1990;39:408–411.
34. Zhou X, Pardue MT, Iuvone PM, Qu J. Dopamine signaling and myopia development: what are the key challenges. *Prog Retin Eye Res*. 2017;61:60–71.
35. Nickla DL, Yusupova Y, Totonelly K. The muscarinic antagonist MT3 distinguishes between form deprivation- and negative lens-induced myopia in chicks. *Curr Eye Res*. 2015;40:962–967.
36. Ashby RS, Schaeffel F. The effect of bright light on lens compensation in chicks. *Invest Ophthalmol Vis Sci*. 2010;51: 5247–5253.
37. Smith EL III, Hung LF, Arumugam B, Huang J. Negative lens-induced myopia in infant monkeys: effects of high ambient lighting. *Invest Ophthalmol Vis Sci*. 2013;54:2959–2969.
38. Smith EL III, Hung LF, Huang J. Protective effects of high ambient lighting on the development of form-deprivation myopia in rhesus monkeys. *Invest Ophthalmol Vis Sci*. 2012; 53:421–428.
39. Nickla DL, Totonelly K. Choroidal thickness predicts ocular growth in normal chicks but not in eyes with experimentally altered growth. *Clin Exp Optom*. 2015;98:564–570.
40. Sonoda S, Sakamoto T, Yamashita T, et al. Choroidal structure in normal eyes and after photodynamic therapy determined by binarization of optical coherence tomographic images. *Invest Ophthalmol Vis Sci*. 2014;55:3893–3899.
41. Esmaeelpour M, Kajic V, Zabihian B, et al. Choroidal Haller's and Sattler's layer thickness measurement using 3-dimensional 1060-nm optical coherence tomography. *PLoS One*. 2014;9: e99690.
42. Tan CS, Cheong KX. Macular choroidal thicknesses in healthy adults—relationship with ocular and demographic factors. *Invest Ophthalmol Vis Sci*. 2014;55:6452–6458.
43. Read SA, Alonso-Caneiro D, Vincent SJ, Collins MJ. Longitudinal changes in choroidal thickness and eye growth in childhood. *Invest Ophthalmol Vis Sci*. 2015;56:3103–3112.
44. Hsu CC, Huang N, Lin PY, et al. Prevalence and risk factors for myopia in second-grade primary school children in Taipei: a population-based study. *J Chin Med Assoc*. 2016;79:625–632.
45. Woodman-Pieterse EC, Read SA, Collins MJ, Alonso-Caneiro D. Regional changes in choroidal thickness associated with accommodation. *Invest Ophthalmol Vis Sci*. 2015;56:6414–6422.
46. Chiang ST, Phillips JR. Effect of atropine eye drops on choroidal thinning induced by hyperopic retinal defocus. *J Ophthalmol*. 2018;2018:8528315.
47. Jin P, Zou H, Zhu J, et al. Choroidal and retinal thickness in children with different refractive status measured by swept-source optical coherence tomography. *Am J Ophthalmol*. 2016;168:164–176.
48. Nagasawa T, Mitamura Y, Katome T, et al. Macular choroidal thickness and volume in healthy pediatric individuals measured by swept-source optical coherence tomography. *Invest Ophthalmol Vis Sci*. 2013;54:7068–7074.
49. Chhablani JK, Deshpande R, Sachdeva V, et al. Choroidal thickness profile in healthy Indian children. *Indian J Ophthalmol*. 2015;63:474–477.
50. Al-Haddad C, El Chaar L, Antonios R, El-Dairi M, Noureddin B. Interocular symmetry in macular choroidal thickness in children. *J Ophthalmol*. 2014;2014:472391.
51. Read SA, Collins MJ, Vincent SJ, Alonso-Caneiro D. Choroidal thickness in childhood. *Invest Ophthalmol Vis Sci*. 2013;54: 3586–3593.


Investigative Ophthalmology & Visual Science